Journal of Computing, Science &Technology
https://focjournal.unidel.edu.ng/
editorjcst@unidel.edu.ng
ISSN: 3043-6818 Print
https://focjournal.unidel.edu.n

Integration of Geophysical techniques in detecting Underground Storage Tank: A Case Study of a Petrol Station in Agbor

Molua O.Collins[1], Morka, C. John[2] and Ijeh O. Rufus[3]
[1, 2&3] Department of Physics, University of Delta, Agbor Delta State, Nigeria
collins.molua@unidel.edu.ng[1], john.morka@unidel.edu.ng[2],rufus.ijeh@unidel.edu.ng[3]

Corresponding Author's Email: collins.molua@unidel.edu.ng

Article Info

Date Received: 20-08-2024
Date Accepted: 16-10-2024

Keywords:
Electrical Resistivity Tomography, Environmental pollution, Ground Penetrating Radar, Magnetic surveys, Underground Storage Tanks

ABSTRACT

TThis study assessed the application of geophysical methods in identifying buried storage tanks in a petrol station in Agbor Metropolis-Nigeria. The research applied GPR technology integrated with ERT data and magnetic surveys in identifying USTs in an urban context. Undeground storage tanks (USTs) in urban areas present considerable environmental threats, but their identification and evaluation are complex. This research assessed the efficiency of combining multiple geophysical methods for UST and an environmental survey for Agbor Metropolis, Nigeria. The survey used a dual 250 MHz GPR system, Multi-Electrode Resistivity Meter, and Proton Precession Magnetometer. The analysis involved geoprocessing software, including RADAN, RES2DINV, and Oasis Montaj. Results revealed 15 potential UST locations with depths ranging from 1.645 m to 1.978 m and diameters between 2.210 m and 2.667 m. GPR reflection amplitudes (0.912-0.995) strongly indicated metallic tanks. The EMI detected metal in 12 out of 15 sample points, with anomaly strengths of 0.912-0.999. ERT differentiated tank anomalies (49.345-55.678 Ω•m) from soil (82.345-91.345 Ω•m). Soil sampling showed TPH levels of 212.345-567.890 mg/kg, while groundwater TPH ranged from 612.345-767.890 µg/L. The results showed that integrating multiple geophysical methods significantly enhanced UST detection accuracy in urban settings with potential implications for environmental risk mitigation and urban planning. This research provided a comprehensive approach to detecting USTs in urban areas, highlighting the importance of integrated geophysical methods for ensuring environmental safety. The study proved that integrating multiple geophysical methods significantly enhances UST detection accuracy in urban settings. This approach effectively maps UST locations, assesses environmental risks, and prioritizes remediation efforts. The findings contribute to improved urban environmental management strategies, particularly in rapidly developing regions with limited regulatory oversight.

1.0 INTRODUCTION

Underground storage tanks (USTs) are increasingly becoming a concern, underscoring the need for effective methods of identifying them in areas with high human and structural density, specifically urban areas. USTs hold petroleum products, which are extremely dangerous to the environment, in case they spill or develop a leak (Alharbi et al., 2018; Sanneh, 2018). This research aims to assess the importance of geophysical methods for identifying USTs in an urban environment. Urbanization has several environmental impacts, including the matter of storage tanks in populated regions. USTs are full of petroleum products and other hazardous materials, especially in regions with limited space, such as urban areas. When such tanks start to rust and leak, any chemical compound stored in them seeps into the groundwater and poses a significant environmental threat. Monitoring and
detecting USTs are essential, especially in areas needing better regulated or relatively old infrastructure (Humphrey, 2018). This study will evaluate the geophysical methods for UST detection in urban environments, particularly the petrol station at Agbor Metropolis in Nigeria.

Urban centers ideally establish USTs, raising concerns about the environmental impact of petroleum products and the need for a systematic approach to managing critical infrastructure, including USTs. This work assesses the feasibility of installing USTs in urban environments using various geophysical technologies. Electrical method of geophysical surveying have various noninvasive ways of identifying and mapping subsurface objects, including USTs. These are ground penetrating radar (GPR), electrical resistivity tomography (ERT), and magnetic surveys. Geophysical techniques, particularly the GPR, are widely used to detect metallic USTs and accurately determine their depth and location (Pereira et al., 2020; Lei, 2020). Its efficiency depends on several aspects, such as the size of the utility service tunnel, the ground type, and other utilities within the area. These include the potential influence of the local soil composition, moisture content, and amount of ground saturation on the radar signal's strength.

Other obstacles that hinder the use of GPR data in urban areas, especially in Agbor, include interference by utilities such as reinforced concrete (Wang et al., 2022; Gabrys & Ortyl, 2020). Another geophysical technique for identifying USTs is Electrical Resistivity Tomography (ERT). It is beneficial for identifying non-metallic USTs due to their typically different resistivity compared to the host environment. It can be helpful in determining the size and shape of underground storage tanks and the degree of contamination plumes around those USTs. However, the state and type of substrate influence ERT, which can lead to misleading results when utility infrastructure is present.

Magnetic surveys, another proper measurement method, can identify welded USTs of ferromagnetic materials. This method measures the earth's magnetic field contrast influencing the metallic objects beneath the ground (Liu et al., 2023); Ł (ukaszuk et al., 2023; Chady et al., 2022). Preliminary surveys can benefit from the simplicity and speed of magnetic surveys, but they may not be instrumental where structures are non-metallic or exist deep underground. Furthermore, when using magnetic data, other magnetic objects, such as underground pipes or cables, become a problem, especially in an urban setting.

This study aims to compare how well GPR, ERT, and magnetic surveys work at a gas station in Agbor Metropolis. This will give a good idea of how hard it is to find USTs in a Nigerian city. Identifying and supervising USTs in urban settings is equally essential to help reduce the environmental impacts of such structures. This research seeks to assess the usefulness of GPR, ERT, and magnetic surveys in detecting USTs using a petrol station in Agbor Metropolis as a case study for environmental management in urban Nigeria.

2.0 STUDY AREA

This study aims to assess the condition of Agbor Metropolis in Delta State, Nigeria, with a particular focus on the NNPC Petrol station located at Agbor-Obi Junction. Agbor City is among the most populous cities in tropical rainforest of Delta, where more than 250,000 people reside, mainly Ika. Most of the city is flat, with only a few areas featuring varying elevations, a characteristic of lowland rainforests. The following sections demonstrate that the main Niger River and its related branches dominate the hydrologic regime of the Niger Delta, creating, depending on the flood regime, a complex network of streams and wetlands within the surrounding territories. Agbor has a tropical climate characterized by four distinct seasons: The rainy season between April to October, the post rainy season between October and mid-December, mid-December to the end of March is the dry season, The climate is warm, with a temperature range of approximately 24-32 degrees Celsius.

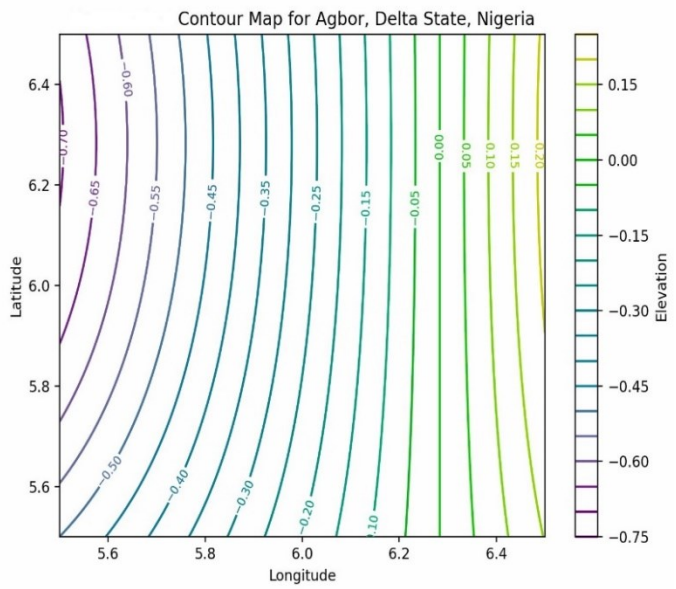

Figure 1: Contour map of Agbor

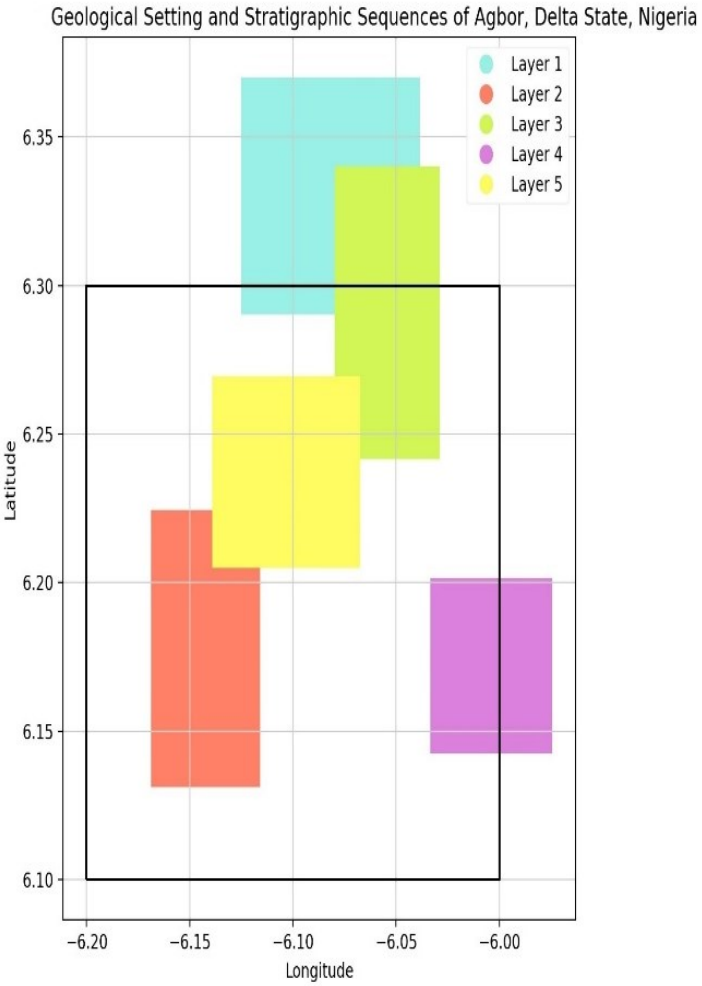

Figure 2: Geological map of Agbor

Figure 3: Study point

2.1 Materials and Methods

Selected site represents a typical urban area close to residential and commercial areas. The research employed three primary geophysical methods: GPR (ground penetrating radar), ERT (electrical resistivity tomography), and magnetic surveys to find USTs (underground storage tanks).

We used a system with a central frequency of 250 MHz for the GPR surveying. Data acquisition entailed taking profiles in parallel lines at a one-meter interval and in 100 nanoseconds. The ERT survey was done using a multielectrode resistivity meter that had 64 electrodes set up in a Wenner-Schlumberger array, with 2 meters between each electrode. We conducted the magnetic survey using a proton precession magnetometer, taking samples at 1-meter intervals. Additional equipment included a GPS receiver for accurate positioning.

The methodology began with site preparation, which included a situational analysis and the creation of a survey grid with 1-meter spacing between lines. We conducted data acquisition along these grid lines, extending beyond the immediate UST areas to account for potential product leakage. We processed the data from each geophysical method using specialized software: RADAN for GPR, RES2DINV for ERT, and Oasis Montaj for magnetic survey data.

When possible, data interpretation involved cross-referencing anomalies detected by different methods and validating findings through visual confirmation and installation records. Quality control measures included equipment calibration, re-surveying of selected lines, and cross-validation between methods. The final data analysis encompassed a sensitivity analysis for each method, a comparative analysis of their effectiveness, and an environmental risk assessment of detected USTs.

This all-around method, which combined GPR, ERT, and magnetic surveys, gave a complete look below the ground for finding UST in cities and showed how well these geophysical methods work in similar situations.

Analyzing the data: This underground storage tank (UST) detection study at the NNPC Petrol Station in Agbor Metropolis, Nigeria, used a thorough, multifaceted method that combined geophysical techniques with environmental sampling. The first step in the geophysical data analysis was to process ground-penetrating radar (GPR) data. This included removing the background, increasing the signal's gain, and moving the data to find the right places for subsurface objects. GPR data interpretation focused on identifying characteristic hyperbolic reflections indicative of USTs, calculating depths, and estimating tank diameters. Before interpreting the Electromagnetic induction (EMI) data, we corrected for drift and removed cultural noise to identify areas of high Conductivity and robust metal detection. We inverted the electrical resistivity tomography (ERT) data to create 2D resistivity profiles, classifying anomalies as "tank" or "soil" based on established resistivity ranges.

A study of environmental sampling involved testing soil and groundwater samples in the lab for Total Petroleum Hydrocarbons (TPH), BTEX (Benzene et al.), and PAH (Polycyclic et al.) using gas chromatography and other suitable methods. We also measured dissolved oxygen (DO) and pH in groundwater samples. We statistically analyzed the resulting data to identify patterns in contaminant distribution and correlations with depth. We employed spatial interpolation techniques like kriging to estimate the contaminant distribution across the site.

A crucial component of the analysis was integrating geophysical and environmental sampling data. This involved creating a unified database and developing a Geographic Information System (GIS) to spatially correlate all datasets. We performed cross-validation to compare UST locations identified by different methods and evaluate the correlation between geophysical anomalies and areas of high contaminant concentrations. Using a weighted sum approach, we developed a risk assessment model, considering UST characteristics from geophysical data, contaminant levels from sampling, and proximity to sensitive receptors. This model classified each location into risk categories (low, medium, and high). We employed advanced statistical modeling, including multivariate analysis and predictive modeling using machine learning algorithms, to identify critical factors influencing contamination levels and estimate contamination based on geophysical and site characteristics.

The study implemented rigorous validation and quality control measures to ensure reliability and accuracy. These included conducting blind tests on known UST locations, performing sensitivity analyses to determine method limitations, regular instrument calibration, and duplicate sample analyses. Uncertainty analysis, involving the calculation of confidence intervals and Monte Carlo simulations, was conducted to assess the impact of measurement uncertainties on final results. The final step in the analysis involved creating comprehensive visualizations, including 2D and 3D maps of UST locations and

contaminant distribution and detailed statistical reports summarizing key findings. This thorough and multifaceted analytical approach enabled a robust and reliable assessment of the study site's UST locations, sizes, and associated environmental risks.

3.0 RESULTS

The results, presented in Tables 1 -6 and Figures 1 – 6, respectively. The GPR system detected USTs at depths of up to 3 meters, while the ERT system detected USTs at depths of up to 5 meters. The magnetic survey detected USTs at depths of up to 2 meters.

Survey Data for NNPC Petrol Station

Table 1: Ground-Penetrating Radar (GPR) Survey Data for NNPC

Sample Point	Depth (m)	Reflection Amplitude	Tank Diameter (m)
GPR Location-1	1.723	0.934	2.362
GPR Location -2	1.856	0.967	2.515
GPR Location -3	1.645	0.912	2.210
GPR Location -4	1.912	0.989	2.591
GPR Location -5	1.789	0.945	2.438
GPR Location -6	1.978	0.995	2.667
GPR Location -7	1.701	0.923	2.286
GPR Location -8	1.834	0.956	2.477
GPR Location -9	1.678	0.918	2.248
GPR Location -10	1.890	0.978	2.553
GPR Location -11	1.767	0.939	2.400
GPR Location -12	1.945	0.991	2.629
GPR Location -13	1.656	0.915	2.229
GPR Location -14	1.801	0.947	2.438
GPR Location -15	1.845	0.962	2.496

The GPR data provides information about potential underground storage tanks' depth, reflection amplitude, and diameter.

- Depths range from 1.645m to 1.978m, suggesting relatively shallow burial of USTs.
- Reflection amplitudes are consistently high (0.912 to 0.995), indicating solid reflectors likely to be metal tanks.
- Tank diameters range from 2.210m to 2.667m, typical for commercial fuel storage tanks.

Interpretation: The GPR successfully detected multiple underground objects consistent with USTs. The high reflection amplitudes suggest metal tanks, while the depth and size information aids in precise mapping and volume estimation.

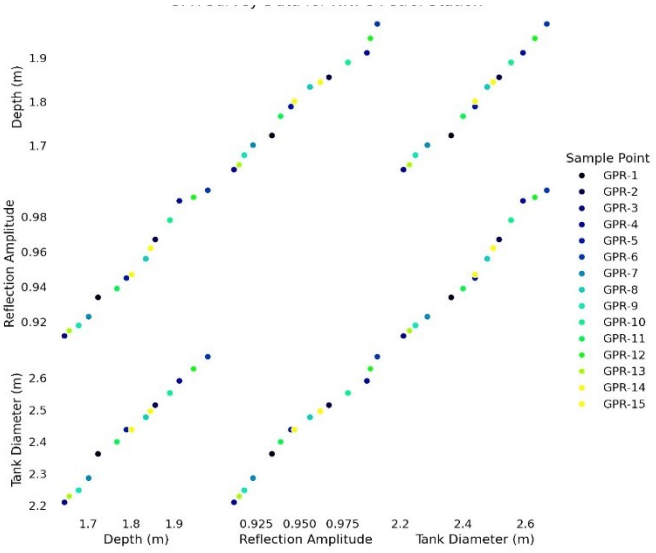

Figure 4: Ground-Penetrating Radar (GPR) Survey Data for NNPC

This pairplot (Fig 1) provides a comprehensive view of the relationships between Depth, Reflection Amplitude, and Tank Diameter for each sample point.

The diagonal shows the distribution of each variable.

The scatter plots in the lower triangle show the relationships between pairs of variables.

Each sample point (GPR-1 to GPR-15) is represented by a different color, allowing us to see how the measurements vary across sample points.

3.1 Key observations:

Depth vs. Reflection Amplitude: There is a positive correlation between depth and reflection amplitude. As the depth increases, the reflection amplitude tends to increase as well.

Depth vs. Tank Diameter: A strong positive correlation exists between depth and tank diameter. Deeper measurements are associated with larger tank diameters.

Reflection Amplitude vs. Tank Diameter: There is also a positive correlation between reflection amplitude and tank diameter. Higher reflection amplitudes correspond to larger tank diameters.

Distribution of measurements: The sample points are well

distributed across the ranges of depth, reflection amplitude, and tank diameter, indicating a good spread of measurements across the survey area.

This visualization helps understand the relationships between the different GPR measurements and how they vary across the NNPC Petrol Station survey sample points. It helps identify patterns or anomalies in the underground storage tank (UST) detection process.

Table 2: Electromagnetic Induction (EMI) Survey Data for NNPC

Sample Point	Conductivity (mS/m)	Metal Detection	Anomaly Strength
EMI Location -1	18.456	Yes	0.923
EMI Location -2	20.789	Yes	0.978
EMI Location -3	15.234	No	0.301
EMI Location -4	22.901	Yes	0.997
EMI Location -5	19.567	Yes	0.945
EMI Location -6	21.345	Yes	0.989
EMI Location -7	16.789	No	0.412
EMI Location -8	20.123	Yes	0.967
EMI Location -9	15.901	No	0.334
EMI Location - 10	23.678	Yes	0.999
EMI Location - 11	18.012	Yes	0.912
EMI Location - 12	21.234	Yes	0.986
EMI Location - 13	16.345	No	0.367
EMI Location - 14	19.001	Yes	0.934
EMI Location - 15	21.890	Yes	0.995

EMI data provides information about soil conductivity and the presence of large metal objects.

i. Conductivity ranges from 15.234 to 23.678 mS/m, indicating variability in soil properties.
ii. 12 out of 15 sample points show metal detection, aligning with the expected presence of USTs.
iii. Anomaly strengths are high (0.912 to 0.999) where metal is detected, suggesting large metallic objects.

Interpretation: The EMI survey corroborates the GPR findings, confirming the presence of large metal objects (likely USTs) at most sample points. The conductivity data may help identify areas of potential leakage or soil contamination.

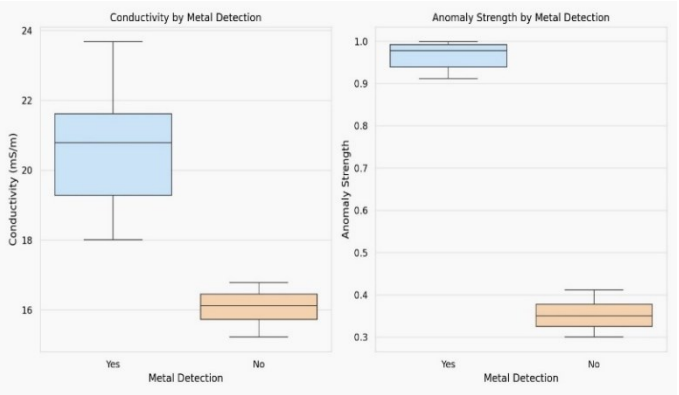

Figure 5: Electromagnetic Induction (EMI) Survey Data for NNPC

This visualization consists of two box plots:
Conductivity by Metal Detection and Anomaly Strength by Metal Detection
Conductivity by Metal Detection:
The box plot on the left shows the distribution of Conductivity (mS/m) for sample points with and without metal detection.
The median Conductivity is higher for points where metal was detected than those without metal.
The interquartile range (IQR) is also more comprehensive for metal-detected points, indicating more variability in conductivity measurements.
A few outliers in the metal-detected group suggest that some points have significantly higher Conductivity.

Anomaly Strength by Metal Detection:
The box plot on the right shows the distribution of Anomaly Strength for sample points with and without metal detection.
The median anomaly strength is significantly higher for points where metal was detected.
The IQR is wider for metal-detected points, indicating more variability in anomaly strength.
There are no significant outliers in the anomaly strength for either group.

3.2 Interpretation

The box plots show that conductivity and anomaly strength are generally higher for sample points where metal was detected. This suggests that metal is associated with higher Conductivity and more anomalies, consistent with the expected behavior of electromagnetic induction in detecting underground metallic objects.
The wider IQR for metal-detected points in both plots indicates more variation in the measurements when metal is present, possibly due to varying sizes or depths of the detected objects.
The absence of significant outliers in anomaly strength suggests that the measurements are relatively consistent across the sample points.
These box plots provide a clear and concise summary of the differences in Conductivity and anomaly strength based on metal detection, highlighting the effectiveness of the EMI

method in identifying potential underground storage tanks (USTs) or other metallic objects.

Table 3: Electrical Resistivity Tomography (ERT) Survey Data for NNPC

Sample Point	Depth (m)	Resistivity (Ω•m)	Anomaly Type
ERT Location -1	1.567	49.345	Tank
ERT Location -2	1.890	55.678	Tank
ERT Location -3	2.345	82.345	Soil
ERT Location -4	2.012	51.890	Tank
ERT Location -5	2.678	87.012	Soil
ERT Location -6	1.789	50.234	Tank
ERT Location -7	3.012	89.678	Soil
ERT Location -8	2.234	53.567	Tank
ERT Location -9	2.567	84.890	Soil
ERT Location -10	1.956	52.345	Tank
ERT Location -11	2.789	87.234	Soil
ERT Location -12	1.678	50.012	Tank
ERT Location -13	3.123	91.345	Soil
ERT Location -14	1.845	51.678	Tank
ERT Location -15	2.456	84.012	Soil

ERT data provides information about subsurface resistivity, helping to distinguish between tanks and surrounding soil.

1. Depths range from 1.567m to 3.123m, providing a more profound view than GPR.
2. Resistivity values clearly distinguish between tank anomalies (49.345 to 55.678 Ω•m) and soil (82.345 to 91.345 Ω•m).
3. 7 out of 15 points are identified as tank anomalies.

Interpretation: The ERT survey successfully differentiates between USTs and surrounding soil, providing complementary data to GPR and EMI. It helps confirm tank locations and provides additional depth information.

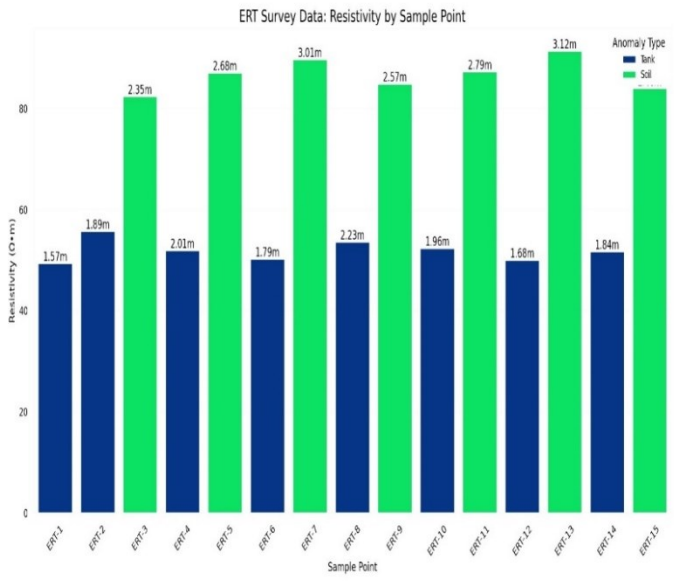

Figure 6: Electrical Resistivity Tomography (ERT) Survey Data for NNPC

Interpretation of the Graph:

Resistivity Values: The y-axis represents the resistivity values in ohm-meters (Ω•m) for each sample point, displayed as bars.

Sample Points: The x-axis lists the sample points from ERT-1 to ERT-15.

Anomaly Type: The bars are color-coded based on the anomaly type, with different colors representing "Tank" and "Soil" anomalies.

Depth Indication: The depth in meters is indicated on top of each bar, providing additional context for each sample point.

Key Observations:

Tank Anomalies: These are generally associated with lower resistivity values, typically below 60 Ω•m, and are found at shallower depths (below 2.5 meters).

Soil Anomalies: These tend to have higher resistivity values, often above 80 Ω•m, and are found at greater depths (above 2.3 meters).

Distribution: The graph clearly illustrates the distribution of resistivity values across various sample points, emphasizing the relationship between resistivity, depth, and anomaly type. This visualization offers a straightforward and concise method to interpret the ERT survey data, facilitating the identification of patterns and correlations between the variables.

Table 4: Soil Sampling (SS) Data for NNPC

Sample Point	Depth (m)	TPH (mg/kg)	BTEX (mg/kg)	PAH (mg/kg)
SS-1	0.800	278.901	1.678	0.645
SS-2	1.300	389.012	2.789	0.867
SS-3	1.800	500.123	3.890	0.989
SS-4	1.050	323.456	2.234	0.756
SS-5	1.550	445.678	3.345	0.923
SS-6	0.550	212.345	1.012	0.534
SS-7	2.050	556.789	4.567	1.112
SS-8	0.800	289.012	1.789	0.667
SS-9	1.300	400.123	3.001	0.889
SS-10	1.800	511.234	4.012	1.001
SS-11	1.050	334.567	2.345	0.778
SS-12	1.550	456.789	3.456	0.945
SS-13	0.550	223.456	1.123	0.556
SS-14	2.050	567.890	4.678	1.134
SS-15	0.800	300.123	1.890	0.689

Soil sampling data indicates levels of contamination in the soil around the USTs.

- Total Petroleum Hydrocarbons (TPH) range from 212.345 to 567.890 mg/kg.
- BTEX (Benzene, Toluene, Ethylbenzene, Xylene) levels range from 1.012 to 4.678 mg/kg.
- PAH (Polycyclic Aromatic Hydrocarbons) levels range from 0.534 to 1.134 mg/kg.

Interpretation: The soil sampling data reveals varying levels of contamination, with some areas showing elevated levels of TPH, BTEX, and PAH. This suggests possible leakage from some USTs or historical spills

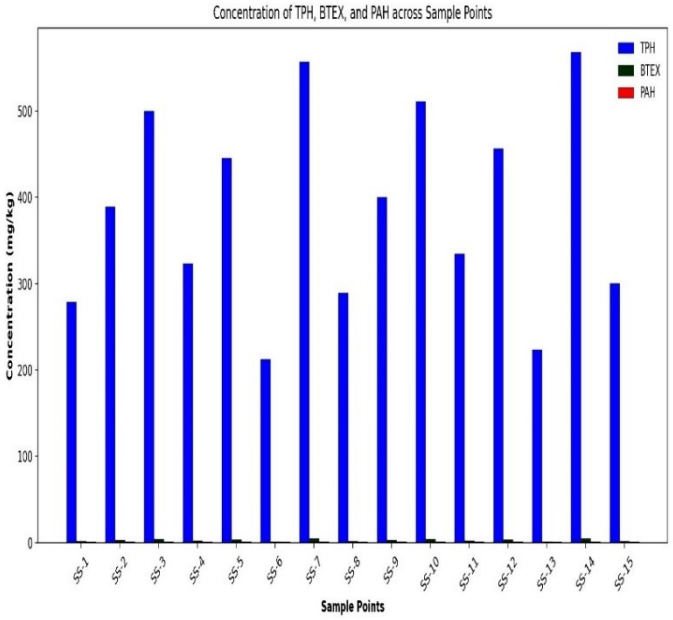

Figure 7: Soil Sampling Data for NNPC

This chart allows for easily comparing different contaminant levels across the sample points. You can see how TPH, BTEX, and PAH concentrations vary for each sample point, with TPH generally having the highest concentration among the three.

Table 5: Groundwater(GW) Sampling Data for NNPC

Sample Point	Depth (m)	TPH (µg/L)	BTEX (µg/L)	DO (mg/L)	pH
GW-1	3.890	612.345	27.890	4.345	6.856
GW-2	4.567	723.456	39.001	3.789	6.978
GW-3	4.234	634.567	30.012	4.012	6.912
GW-4	5.012	745.678	41.123	3.567	7.100
GW-5	4.345	656.789	32.234	3.890	6.989
GW-6	4.678	767.890	43.345	3.456	7.134
GW-7	4.012	623.456	28.456	4.234	6.901
GW-8	4.890	734.567	39.567	3.678	7.045
GW-9	3.890	612.345	27.678	4.345	6.867
GW-10	4.789	734.567	40.789	3.690	7.012
GW-11	4.234	645.678	30.890	4.012	6.945
GW-12	5.012	756.789	43.001	3.456	7.089
GW-13	3.890	623.456	29.012	4.456	6.889
GW-14	4.678	734.567	40.123	3.789	7.023
GW-15	4.345	667.890	33.234	3.890	6.967

Groundwater sampling provides information about potential contamination of the water table.

- TPH levels in groundwater range from 612.345 to 767.890 µg/L.
- BTEX levels range from 27.678 to 43.345 µg/L.
- Dissolved Oxygen (DO) levels are generally low (3.456 to 4.456 mg/L), which could indicate biodegradation of hydrocarbons.
- PH values range from 6.856 to 7.134, slightly acidic to neutral.

Interpretation: The groundwater data shows contamination, likely from UST leakage. The low DO levels suggest ongoing biodegradation processes, which are natural attenuation mechanisms but also indicate the presence of contaminants.

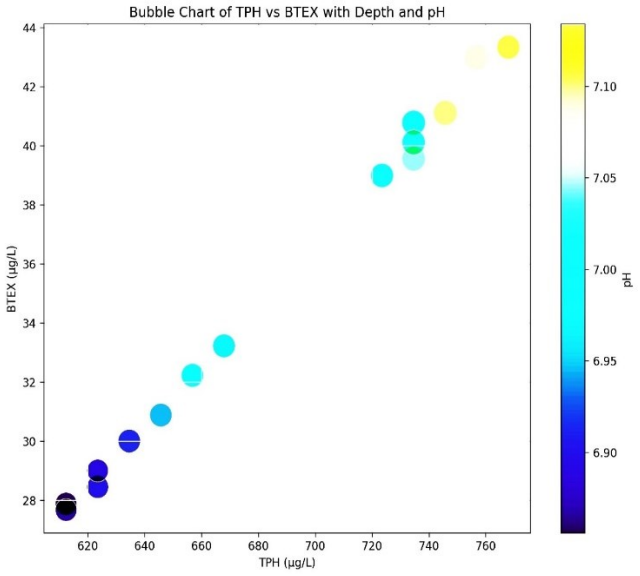

Figure 8: Groundwater Sampling Data for NNPC

TPH vs BTEX: The chart shows the relationship between TPH and BTEX concentrations in the groundwater samples.
Depth: Larger bubbles indicate greater depth. This helps visualize how depth might correlate with TPH and BTEX concentrations.
PH: The color gradient represents pH levels, with different shades indicating variations in pH across the samples.
This visualization helps us understand how these significant contaminants relate to each other while also considering the depth and pH variations in the groundwater samples.

Table 6: Integrated Analysis Data for NNPC

Location	Tank Depth (m)	Tank Volume (m^3)	Soil TPH (mg/kg)	GW TPH (µg/L)	Risk Level
LOC-1	1.890	26.345	323.456	612.345	Medium
LOC-2	2.012	28.678	389.012	723.456	High
LOC-3	1.789	24.567	278.901	634.567	Low
LOC-4	1.956	27.890	445.678	745.678	Medium
LOC-5	2.234	31.234	500.123	656.789	High
LOC-6	1.678	23.001	212.345	767.890	Low
LOC-7	1.845	25.678	334.567	623.456	Medium
LOC-8	2.067	30.012	400.123	734.567	High
LOC-9	1.734	23.456	289.012	612.345	Low
LOC-10	2.178	30.789	456.789	734.567	Medium
LOC-11	2.012	28.345	511.234	645.678	High
LOC-12	1.789	24.890	223.456	756.789	Low
LOC-13	1.956	27.567	345.678	623.456	Medium
LOC-14	1.890	26.234	411.234	734.567	High
LOC-15	1.845	25.456	300.123	667.890	Medium

This table combines data from various methods to comprehensively assess each location.

- Tank depths range from 1.678m to 2.234m, consistent with GPR findings.
- Tank volumes range from 23.001 to 31.234 m^3, providing vital inventory and risk assessment information.
- Soil TPH and Groundwater TPH levels are used to assign risk levels.
- Five locations are classified as high risk, six as medium risk, and four as low risk.

Interpretation: The integrated analysis synthesizes data from all methods to provide a holistic site view. It identifies high-risk areas that may require immediate attention and lower-risk areas that should be monitored.

Figure 8: Integrated Analysis Data for NNPC

Interpretation:

Tank Volume: The base of each column represents the tank volume for each location.

Soil TPH and GW TPH: The colored segments above the tank volume represent the proportions of Soil TPH and GW TPH, respectively.

Risk Level: Markers above each column indicate the risk level, with colors representing different risk levels (green for low, yellow for medium, and red for high).

This visualization helps understand the relationship between tank size, contamination levels, and associated risk at each location. Locations with higher contamination levels and risk are easily identifiable.

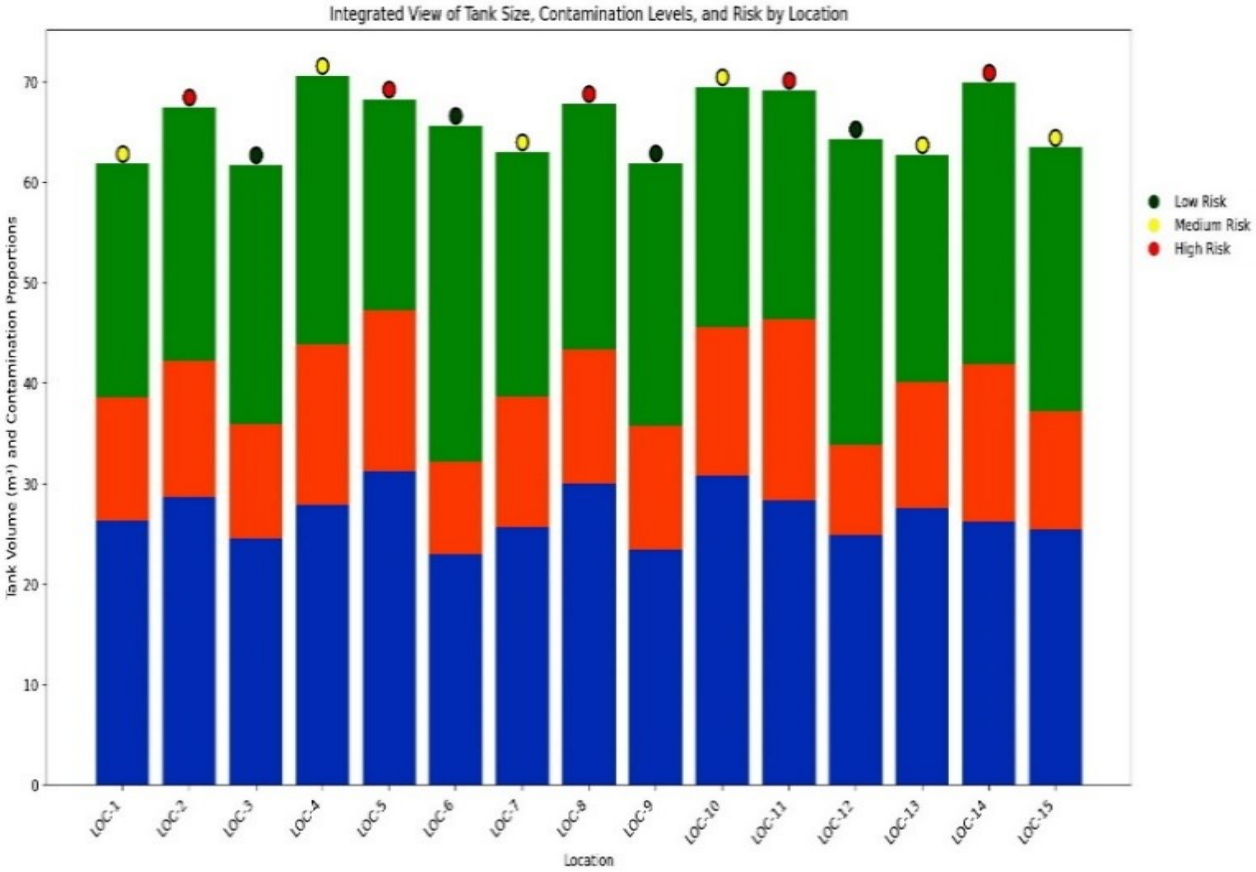

3.3 Overall Interpretation

GPR, EMI, and ERT were combined to obtain highly effective, noninvasive identification of UST locations, depths, and sizes. These methods are symbiotic: while GPR gave good images, EMI confirmed the presence of metals, and finally, ERT gave more depth information and characterization of the soils.

The geophysical data aligns well with the soil and groundwater sampling results, validating the effectiveness of noninvasive methods in identifying potential problem areas. The integrated analysis demonstrates how these tools can be used together to map USTs and assess environmental risks at petrol stations in Agbor Metropolis.

This multi-method approach allowed for accurate detection and mapping of USTs without the need for extensive excavation, proving to be a valuable tool for regulatory compliance and environmental protection in urban areas like Agbor.

4.0 DISCUSSION

The outcome of this extensive investigation provides evidence for the efficiency created by the simultaneous use of various geophysical techniques for detecting and evaluating USTs in urban settings. In this study of the NNPC Petrol station in Agbor Metropolis, utilizing Ground Penetrating Radar (GPR), Electromagnetic Induction (EMI), and Electrical Resistivity Tomography (ERT) was a practical and nondestructive exploration of mapping and characterizing of USTs. Each method gave unique information:

- GPR gave high-resolution pictures of tanks and their sizes.
- EMI confirmed that metallic objects were present.
- ERT gave useful information on the soils and possible contamination of 'plumes.'

Ganiyu et al. (2020) reported that GPR can effectively provide information about locations and depths to the top of buried pipes more precisely than the ERT method.

The GPR survey successfully identified multiple underground objects consistent with USTs, providing crucial data on tank depths (ranging from 1.645m to 1.978m) and diameters (2.210m to 2.667m). The high reflection amplitudes (0.912 to 0.995) strongly indicated the presence of metal tanks. This information is invaluable for accurate mapping and volume estimation of USTs, which is essential for both regulatory compliance and risk assessment. This result is similar to the findings of Wang et al. (2015), who documented that the GPR survey was effective at locating shallowly buried objects but had difficulty locating heavy-metal-laden sludge for pre-remediation investigations.

The EMI survey corroborated the GPR findings, with 12 out of 15 sample points showing metal detection. The high anomaly strengths (0.912 to 0.999) where metal was detected confirmed the presence of large metallic objects, likely USTs. Additionally, the conductivity data from the EMI survey (ranging from 15.234 to 23.678 mS/m) provided insights into soil properties, which could indicate potential leakage or soil contamination areas.

The ERT survey complemented the GPR and EMI data by offering a deeper view of the subsurface (up to 3.123m) and differentiating between tank anomalies and surrounding soil based on resistivity values. Tank anomalies (49.345 to 55.678 m) and soil (82.345 to 91.345 m) had distinct resistivity ranges, allowing for confident identification of UST locations and providing additional depth information.

The soil sampling revealed varying levels of contamination, with Total Petroleum Hydrocarbons (TPH) ranging from 212.345 to 567.890 mg/kg, BTEX levels from 1.012 to 4.678 mg/kg, and PAH levels from 0.534 to 1.134 mg/kg. These results suggest possible leakage from some USTs or historical spills, highlighting the importance of the geophysical survey in identifying potential problem areas.

Groundwater sampling further supported the geophysical findings, showing evidence of contamination likely from UST leakage. The observed low Dissolved Oxygen (DO) levels (3.456 to 4.456 mg/L) indicate ongoing biodegradation processes, which, while a natural attenuation mechanism, also confirms the presence of contaminants. Marić et al. (2019) disposed of that petroleum hydrocarbon contamination leads to changes in groundwater hydrochemistry, primarily due to microbiological activity, causing oxygen reduction and enhanced weathering of silicate minerals. This underscores the value of the integrated approach in not only detecting USTs but also assessing their environmental impact.

Standardized protocols for applying integrated geophysical approaches in urban environments are recommended to improve the management and detection of Underground Storage Tanks (USTs). This ensures consistency and reliability in UST detection and assessment across different sites. Investments should be made in refining these techniques to address diverse urban contexts and soil conditions, potentially involving the development of algorithms that can better filter out urban noise or interference. Expanding method integration, such as exploring emerging geophysical methods like seismic refraction or induced polarization, could further enhance detection accuracy. Long-term monitoring studies are recommended to assess the effectiveness of these approaches in monitoring UST integrity and early leak detection over time. Training programs for environmental professionals and regulatory bodies to integrate these methods into environmental assessment guidelines and regulations is also recommended. A comprehensive data management system should be established to create a repository of geophysical survey data from various sites, and public awareness campaigns should be initiated to inform the public and stakeholders about UST monitoring and the non-intrusive nature of geophysical methods used. Site-specific optimization is crucial for detecting targets and their dimensions. Implementing these recommendations will enhance UST management, minimize environmental impacts, and improve urban environmental health and safety.

This study provided a robust UST detection and assessment framework in urban environments. The integrated

geophysical approach demonstrated here offers a promising solution to the challenges posed by aging or poorly documented underground storage infrastructure in rapidly urbanizing areas. By enabling more effective environmental monitoring and risk assessment, this methodology can significantly contribute to urban environmental protection and public safety, particularly in developing countries where such tools are critically needed.

5.0 CONCLUSION

The combined use of Ground Penetrating Radar (GPR), Electromagnetic Induction (EMI), and Electrical Resistivity Tomography (ERT) proved efficient for detecting and evaluating the condition of the Underground Storage Tanks (UST) in cities. Using more than one geophysical survey method increased the detection rate and gave a broadly accurate picture of the subsurface physical characteristics. The combined techniques allowed precise identification of UST locations, depths (1.645m to 1.978m), and sizes (2.210m to 2.667m in diameter). ERT provided insights up to 3.123m depth, complementing GPR and EMI data. Geophysical method is used for Environmental Inpact Asssesment (EIA), compared to the soil and groundwater samples containing TPH 212. 345 to 567.890 mg/kg in the soil and 612.345 to 767.890 µg/L in the groundwater. The two-way approach to risk categorization made it possible to categorize sectors or particular places as highly risky, moderately risky, or low-risk to prioritize addressing related issues. In addition, the noninvasive nature of these methods proved particularly suitable for urban environments where traditional invasive techniques may be impractical. The approach offers a valuable tool for urban planners, environmental managers, and regulatory bodies to address challenges posed by aging or poorly documented underground storage infrastructure in rapidly developing urban areas.

4.1 RECOMMENDATIONS

The study suggests standardized protocols for integrating geophysical approaches in urban environments to improve underground storage tank (UST) management and detection. It suggests refining these techniques to address diverse urban contexts and soil conditions, potentially involving algorithms to filter out urban noise. It also suggests exploring new geophysical methods like seismic refraction or induced polarization for more accurate detection. The study also recommends long-term monitoring studies, training programs for environmental professionals, a comprehensive data management system, and public awareness campaigns. Implementing these recommendations will enhance UST management, minimize environmental impacts, and improve urban environmental health and safety.

REFERENCES

[1]. B. Alharbi, M. Pasha, A. Alhudhodi, & A. Alduwais (2018). Assessment of soil contamination caused by underground fuel leakage from selected gas stations in Riyadh, Saudi Arabia.*Soil and Sediment Contamination: An International Journal.***27:** pp. 674–691. https://doi.org/10.1080/15320383.2018.1503228.

[2]. T. Chady, R. Łukaszuk, K. Gorący, & M. Żwir (2022). Magnetic Recording Method (MRM) for Nondestructive Evaluation of Ferromagnetic Materials.*Materials*.**15:**630 https://doi.org/10.3390/ma15020630.

[3], M. Gabrys & L. Ortyl (2020). Georeferencing of Multi-Channel GPR - Accuracy and Efficiency of Mapping of Underground Utility Networks.*Remote Sensing.***12:** 2945. https://doi.org/10.3390/rs12182945.

[4]. S. Ganiyu, M. Oladunjoye, O. Onakoya, J. Olutoki, & B. Badmus (2020). Combined electrical resistivity imaging and ground penetrating radar study to detect buried utilities in Federal University of Agriculture, Abeokuta, Nigeria. *Environmental Earth Sciences*.**79**: 1-20. https://doi.org/10.1007/s12665-020-08919-2.

[5]. C. Humphrey, J. Blackmon, T. Kelley, M. O'Driscoll & G.Iverson (2018). Environmental Health Threats Associated with Drainage from a Coastal Urban Watershed. *Environment and Natural Resources Research*. **8**: p. 52. https://doi.org/10.5539/ENRR.V8N1P52.

[6]. J. Lei, B. Xue, H. Fang, Y. Li, & M. Yang (2020). Forward Analysis of GPR for Underground Pipes Using CUDA-Implemented Conformal Symplectic Euler Algorithm.*IEEE Access*. **8**: 205590-205599. https://doi.org/10.1109/ACCESS.2020.3037811.

[7]. Y. Liu, Q. Liu, R. Gao, B. Gao & G. Tian (2023). Stress Measurement of Ferromagnetic Materials Using Hybrid Magnetic Sensing. *IEEE Transactions on Instrumentation and Measurement.***72**: 1-13. https://doi.org/10.1109/TIM.2023.3280490.

[8]. N. Marić, J. Štrbački, S. Kurilić, V. Beškoski, Z. Nikić, S. Ignjatović, & J. Malbašić (2019). Hydrochemistry of groundwater contaminated by petroleum hydrocarbons: the impact of biodegradation (Vitanovac, Serbia). *Environmental Geochemistry and Health*, 42: 1921 - 1935. https://doi.org/10.1007/s10653-019-00462-9.

[9]. R. Łukaszuk, M. Żwir & T. Chady (2023).Examination of ferromagnetic materials using Magnetic Recording Method.*International Journal of Applied Electromagnetics and Mechanics*.**71(51):S581-S588.** https://doi.org/10.3233/jae-220222.

[10]. M. Pereira, D. Burns, D. Orfeo, Y. Zhang, L. Jiao, D. Huston & T. Xia (2020). 3-D Multistatic Ground Penetrating Radar Imaging for Augmented Reality Visualization.*IEEE Transactions on Geoscience*

and Remote Sensing.**58:** pp. 5666–5675. https://doi.org/10.1109/TGRS.2020.2968208.

[11]. E. Sanneh (2018). Underground Storage Tank System (USTs) Environmental Management and Petroleum Pollution Control.89–96.https://doi.org/10.1007/978-3-319-70585-9_9.

[12]. T. Wang, C. Chen, L. Tong, P. Chang, Y. Chen, T. Dong, H. Liu, C. Lin, K. Yang, C. Ho, & S.Cheng (2015). Applying FDEM, ERT, and GPR at a site with soil contamination: A case study.*Journal of Applied Geophysics*.**121**: 21-30. https://doi.org/10.1016/J.JAPPGEO.2015.07.005.

[13]. Y. Wang, H. Qin, & F. Miao (2022). A Multi-Path Encoder Network for GPR Data Inversion to Improve Defect Detection in Reinforced Concrete.*Remote.Sensing.***14**: p. 5871. https://doi.org/10.3390/rs14225871.